Tellus SERIES A DYNAMIC METEOROLOGY AND OCEANOGRAPHY
PUBLISHED BY THE INTERNATIONAL METEOROLOGICAL INSTITUTE IN STOCKHOLM

Tellus (2010), 62A, 123–133
Printed in Singapore. All rights reserved

TELLUS

Salinity-dominated thermohaline circulation in sill basins: can two stable equilibria exist?

By JOHAN NILSSON[1]* and GÖSTA WALIN[2], [1]*Department of Meteorology, Stockholm University, SE-10691, Stockholm, Sweden;* [2]*Department of Earth Sciences, Göteborg University, S-40530, Göteborg, Sweden*

(Manuscript received 19 May 2009; in final form 24 November 2009)

ABSTRACT

The dynamics of a salinity-dominated thermohaline circulation in a sill basin is examined using a two-layer model. A prescribed freshwater supply acts to establish a stable stratification, working against a prescribed destabilizing temperature difference. The upper-layer outflow is in geostrophic balance and the upwelling is driven by a fixed energy supply to small-scale vertical mixing. The salinity-dominated flow may have two qualitatively different modes of operation. First, a mixing-limited regime, where the upper layer is shallower than the sill and the flow strength decreases with increasing density difference. Second, an overmixed regime, where the upper layer extends below the sill and the flow strength increases with density difference. Possibly, mixing-limited and overmixed equilibria, with widely different upper-layer depths, can exist for the same external parameters. In such cases, transitions between the two regimes are associated with abrupt changes of the salinity, depth and flow strength. The present results may be of relevance for ocean circulation in glacial climates and for interpretations of marine palaeo data, issues that are briefly discussed in the context of the Arctic Ocean.

1. Introduction

Conceptual models of thermohaline flows play an important role in the theory of the large-scale ocean circulation (see e.g. Walin, 1985; Welander, 1986; Marotzke, 1996, 2000; Longworth et al., 2005; Kuhlbrodt et al., 2007). For thermohaline flows where the thermal- and haline-density differences counteract each other, multiple equilibrium solutions can arise if the relaxation timescales for the temperature and the salinity are different (Stommel, 1961; Welander, 1986; Walin, 1990; Thual and McWilliams, 1992). The essential physics is highlighted when the temperature difference is prescribed and the salinity difference is forced by a prescribed freshwater flux (see e.g. Marotzke, 2000). In this case there are two types of equilibria: a swift thermally dominated flow and a slow salinity-dominated flow.

A critical aspect of simplified thermohaline models is how the flow strength is related to the density difference. In the classical box model of Stommel (1961), the flow strength is assumed to be linearly proportional the density difference. For oceanic applications, however, the flow is generally controlled by geostrophic dynamics and a balance between vertical advection and diffusion of buoyancy, which yields a flow strength that depends on the density difference as well as on the vertical turbulent diffusion (Welander, 1971). A fundamental challenge is that the resulting flow dynamics is sensitive to how the vertical small-scale mixing depends on the density stratification (Lyle, 1997; Huang, 1999; Nilsson and Walin, 2001). If the energy supply to the small-scale vertical mixing is fixed, then the vertical diffusivity decreases with increasing stratification. As a consequence, the circulation will slow down if the density difference is increased. If the vertical diffusivity is taken to be fixed, on the other hand, the flow becomes stronger when the density difference increases (Welander, 1971; Bryan, 1987; Park, 1999; Zhang et al., 1999). The somewhat counter-intuitive dynamics that arise from a stability-dependent vertical diffusivity have been simulated with ocean circulation models in idealized one- and two-hemisphere basins (Huang, 1999; Nilsson et al., 2003; Mohammad and Nilsson, 2006; Marchal et al., 2007). However, the degree to which the nature of the vertical mixing controls the dynamics of the global thermohaline circulation remains essentially an open question (see e.g. Kuhlbrodt et al., 2007). Here, a main issue is the wind-driven upwelling in the Southern Ocean, which acts to reduce the importance of the low-latitude upwelling associated with vertical mixing, and furthermore, suggests a more complicated relation between the strength of the circulation and the density difference (see e.g. Gnanadesikan, 1999; Marshall and Radko, 2006).

It is important to note that the nature of the feedback between flow- and salinity-perturbations, identified by Stommel (1961),

*Corresponding author.
e-mail: nilsson@misu.su.se
DOI: 10.1111/j.1600-0870.2009.00428.x

depends on the relation between the flow and the density difference. In the standard Stommel model, where the flow increases with the density difference, this feedback acts to destabilize the swift thermally dominated regime but to stabilize the slow salinity-dominated regime (Stommel, 1961; Welander, 1986; Marotzke, 1996). The physics becomes radically different if the flow decreases with increasing density difference. Remarkably, the feedback between flow- and salinity-perturbations reverses signs for such a flow. As a result, the feedback now acts to stabilize the thermally dominated regime but to destabilize the salinity-dominated regime (Nilsson and Walin, 2001; Guan and Huang, 2008).

This paper examines the dynamics of a salinity-dominated thermohaline circulation in a semi-enclosed basin such as the Arctic Ocean. The basin receives a net freshwater input, creating a stable salinity stratification, and exchanges water across a sill with the open ocean, which is characterized by higher salinities and temperatures; see Fig. 1. The exchange flow is assumed to be driven by wind and tidal mixing, which deepens the low-salinity surface layer. A critical assumption is that the energy supply to the small-scale vertical mixing in the basin is fixed. The flow is analysed using a slightly modified version of the conceptual two-layer model due to Nilsson and Walin (2001). In the sill-basin model, the salinity-dominated flow has two dynamical regimes: One 'mixing-limited' regime, where the upper layer is shallower than the sill; and one 'overmixed' regime, where the upper layer extends below the sill. A central issue in this study is the dynamics that arises from the influence of the sill in the overmixed regime. Some aspects of the salinity-dominated flow in a mixing-limited regime has been analysed by Guan and Huang (2008) in a two-box model, which includes effects of wind-forced circulation and thermal restoring. Some of their findings will be reviewed and compared with the results of the present model. The presentation is organized as follows. In Section 2, the model is derived and presented. In Section 3, the steady-state properties of the model are examined and limiting cases are discussed. In the concluding section, the present results are discussed in an oceanographic context with applications to the circulation in the Arctic Ocean.

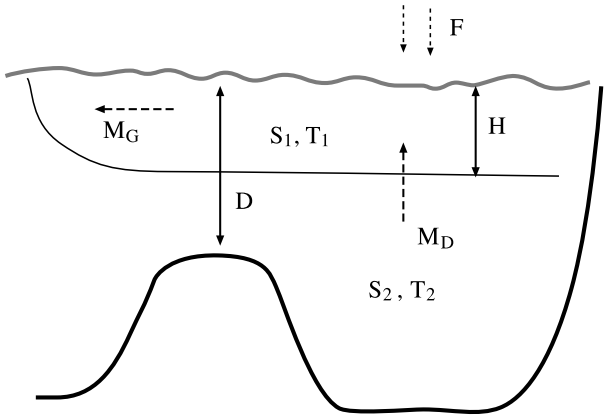

Fig. 1. A sketch of the two-layer model in a semi-enclosed basin, which has a sill depth D. The upper-layer depth H is assumed to be essentially uniform outside narrow boundary currents along the rim of the basin. Here, M_G denotes the horizontal geostrophic exchange flow over the sill, M_D the diapycnal upwelling flow, F the freshwater supply, assumed to be small compared to M_G and M_D . S_1 and T_1 are the upper-layer salinity and temperature, respectively. The lower layer is taken to be a large reservoir with constant salinity and temperature S_2 and T_2. The mixing-limited regime, where $H < D$, is depicted here; see the text for details.

2. A model of salinity-dominated circulation in a sill basin

2.1. Volume and salinity conservation

We consider the conservation of volume and salinity in a semi-enclosed basin, where a surface layer of low-salinity water is floating above a deep homogeneous lower layer, see Fig. 1. The upper/lower layer has the temperature and salinity T_1/T_2 and S_1/S_2, respectively. In the lower layer, the temperature and the salinity are assumed to be given by the conditions in the open ocean. Further, the temperature in the upper layer is assumed to be set by air–sea heat exchange. The depth and the area of the upper layer are denoted H and A, respectively, and its volume is $V = AH$ where A is taken to be constant. Note that the upper-layer depth is assumed to be essentially uniform in the main part of the basin, except for in narrow boundary current along the basin perimeter. The freshwater supply to the upper layer is F, and the geostrophic outflow and the upwelling are denoted M_G and M_D, respectively. Conservation of volume and salinity are given by

$$A\frac{dH}{dt} = -M_G + M_D + F, \tag{1a}$$

$$A\frac{d(HS_1)}{dt} = -S_1 M_G + S_2 M_D. \tag{1b}$$

By combining these two equations, we obtain

$$AH\frac{d\Delta S}{dt} = -\Delta S M_D + (S_2 - \Delta S)F,$$

where $\Delta S = S_2 - S_1$. We assume here that the freshwater supply is small in the sense that $M_G \gg F$ and $M_D \gg F$, which implies that $S_2 \gg \Delta S$. Using this, we arrive at the following approximate conservation relations

$$A\frac{dH}{dt} = -M_G + M_D, \tag{2a}$$

$$AH\frac{d\Delta S}{dt} = -\Delta S M_D + S_2 F. \tag{2b}$$

The density difference is given by

$$\Delta\rho = \rho_0 \beta \Delta S - \Delta\rho_T, \tag{3}$$

where $\Delta\rho_T$ is the density difference associated with the imposed thermal contrast, ρ_0 a constant reference density, and β the haline expansion coefficient. Note that we consider the salinity-dominated regime, for which $\rho_0\beta\Delta S > \Delta\rho_T$.

2.2. Description of the flow

We assume that the exchange flow between the semi-enclosed basin and the open ocean is directly associated the density difference. Hence, we here neglect wind-driven flow components; which effects are briefly discussed in Section 3.3. The classical thermocline scaling (e.g. Welander, 1971; Welander, 1986; Park and Bryan, 2000) is used to derive representations of the flows M_G and M_D. A difference from the standard treatment, which deals with a fixed vertical diffusivity, is that we here use an energy argument due to Kato and Phillips (1969), which yields a vertical diffusivity that decreases with increasing stratification. Straightforward scaling considerations of the thermal wind balance (governing M_G) and the advective diffusive balance (governing M_D) yield (see Nilsson and Walin, 2001; Nilsson et al., 2003, for details)

$$M_G = \frac{g\Delta\rho H^2}{2f\rho_0}, \tag{4}$$

$$M_D = \frac{A\mathcal{E}}{g\Delta\rho H}. \tag{5}$$

Here, g is the acceleration of gravity, f the Coriolis parameter and $\mathcal{E}$ the rate of work per unit area against the buoyancy force associated with the vertical mixing. Note that in order to have a geostrophically controlled exchange flow, the strait connecting the semi-enclosed basin with the open ocean should be wide compared to the internal Rossby radius. For narrow straits, in contrast, the exchange flows tend to be hydraulically controlled (see e.g. Pratt and Spall, 2008).

Implicitly, the flow relations eqs (4) and (5) assume that the upper-layer depth H can vary freely without any constraints imposed by the basin geometry, as long as the upper layer does not approach the bottom. We will now consider how the presence of a sill affects the geostrophic exchange flow. We imagine that the low-saline surface water exits over a sill into a large basin (e.g. from the Arctic Mediterranean into the North Atlantic) as illustrated in Fig. 2. We denote the depth from the sea surface to the sill D. If the upper layer is shallower than the sill, we assume that eq. (4) applies. However, if the upper layer in the basin extends below the sill, the geostrophic outflow is set by the sill depth and the density difference. Accordingly, we assume that the geostrophic flow obeys

$$M_G = \frac{g\Delta\rho H^2}{2f\rho_0}, \quad H < D; \quad M_G = \frac{g\Delta\rho D^2}{2f\rho_0}, \quad H > D. \tag{6}$$

Note that we assume that the diapycnal flow is given by eq. (5) also when the upper layer extends below the sill. When the upper layer is deeper than the sill depth, the situation is similar to that of an overmixed estuary (see e.g. Stommel and Farmer, 1953), as will be discussed later.

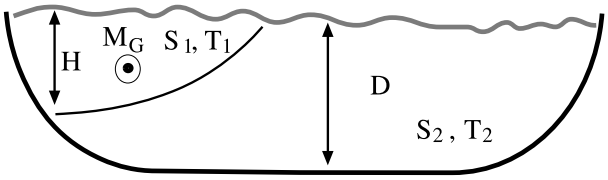

Fig. 2. A cross section in the strait that connects the semi-enclosed basin with the open ocean. The strait, which is assumed to be wide compared to the internal Rossby radius, has a sill with the depth D. The geostrophic outflow from the semi-enclosed basin (M_G) is confined in the upper layer, which has the maximum depth H. Note that H characterize the upstream upper-layer depth, which is uniform over most of the basin. When $H < D$ the flow is in the mixing-limited regime, and when $H > D$ the flow is in the overmixed regime; see the eqs (7a), (7b), (8a) and (8b).

Before proceeding, we will discuss a few issues related to the representation of the geostrophic exchange flow M_G, which entails some implicit assumptions. One central assumptions concerns the contribution from barotropic flow components. If the flow is in geostrophic balance, then the eq. (6) gives the outflow (relative to zero flow at the bottom) in the wedge of the upper layer that not touches the sloping bottom; see Fig. 2. However, there may be a barotropic flow component on the depth contours above the sill level that are within the upper layer (Spall, 2004; Walin et al., 2004; Nilsson et al., 2005). In fact, in the absence of friction an arbitrary barotrotropic flow can be prescribed on closed depth contours (e.g. Greenspan, 1968, section 2.6).[1] In the presence of weak friction, this isobath-following barotropic flow is controlled, in a global fashion, by the wind forcing and the bottom density distribution on the closed depth contours (Nilsson et al., 2005; Aaboe and Nøst, 2008). Here, we assume the presence of a barotropic flow along the depth contours above the sill in the semi-enclosed basin. The strength of the barotropic flow is selected such that it accomplishes the inflow of dense water (assumed to occur on the slope to the right in Fig. 2) and yields zero outflow contribution on the depth contours within the upper layer in the strait. This choice is consistent with the constraint for flows on closed depth contours derived by Nilsson et al. (2005).

Note also that we assume that the volume transport becomes independent of the upper-layer depth when it extends below the sill. Essentially, this follows from the assumption that the outflow on the sill is in geostrophic balance. Based on the thermal wind relation, however, one anticipates that the velocity scale in the semi-enclosed basin should remain proportional H. If the basin velocity scale also characterizes the outflow on the sill, implying departures from geostrophy or an additional barotropic

[1] More generally this applies to closed contours on which the depth divided by the Coriolis parameter are constant.

flow contribution, one would obtain that $M_G \propto HD$ when $H > D$. However, simulations with ocean-circulation models conducted by Walin et al. (2004) and Iovino et al. (2008) suggest that when the upper layer extends below the sill, the exchange flow increases roughly with the square of the sill depth if the density difference remains constant. This motivates us to use the simple relation $M_G \propto D^2$ in this study. We note, however, that the outflow dynamics in situations where the upper-layer depth extends below the sill can be rather complex and frequently involves volume exchange across the sill due to time-dependent baroclinic eddies (Walin et al., 2004; Iovino et al., 2008).

2.3. *Steady-state relations for the flow and the upper-layer depth*

By assuming that $M_G = M_D$ and making use of eqs (5) and (6), we obtain the steady-state dependence of the upper-layer depth and flow strength on the density difference. Note that to also determine the steady-state density difference, we need to consider the salinity balance given by eq. (2b). We denote steady-state quantities with an overbar, and depending on the upper-layer depth there are two different cases.

(i) For $\overline{H} < D$, denoted the mixing-limited regime, we have

$$\overline{H} = \left(\frac{A\mathcal{E}2\rho_0 f}{g^2 \overline{\Delta\rho}^2} \right)^{1/3} \sim \overline{\Delta\rho}^{-2/3}, \tag{7a}$$

$$\overline{M} = \left(\frac{A^2\mathcal{E}^2}{g2\rho_0 f \overline{\Delta\rho}} \right)^{1/3} \sim \overline{\Delta\rho}^{-1/3}. \tag{7b}$$

In this case, the sill is assumed to not affect the dynamics. Note that the flow increases with the vertical mixing, represented by $\mathcal{E}$. Note furthermore that the flow decreases with the density difference. The reason is that geostrophic flow also depends on the upper-layer depth, which becomes greater if the density difference is reduced. As a result, the steady-state flow enhances when the density difference becomes weaker.

(ii) For $\overline{H} > D$, denoted the overmixed regime, we have

$$\overline{H} = \left(\frac{A\mathcal{E}2\rho_0 f}{g^2 \overline{\Delta\rho}^2 D^2} \right) \sim \overline{\Delta\rho}^{-2}, \tag{8a}$$

$$\overline{M} = \frac{g\overline{\Delta\rho}D^2}{2f\rho_0} \sim \overline{\Delta\rho}. \tag{8b}$$

In this case, the mixing is assumed to be sufficiently strong to homogenize the upper layer down below the sill level. Note that the steady-state flow strength, which increases with the density difference, is independent of the vertical mixing energy $\mathcal{E}$. As pointed out by Stommel and Farmer (1953), also the steady-state upper-layer salinity is independent of $\mathcal{E}$ in the overmixed case. This follows from the steady-state salinity balance.

The fact that the steady-state flow in the mixing-limited regime decreases with increasing density difference will prove important for the properties of the model. It is thus relevant to ask if this flow feature is sensitive to our dynamical assumptions. To begin with, we note that for a two-layer flow subjected to hydraulic control, the upper-layer velocity is given by $u = (gH\Delta\rho/\rho_0)^{1/2}$ (e.g. Pratt and Spall, 2008). A straightforward consideration based on a balance between a frictional stress (proportional to the square of the velocity) and the pressure gradient also yields an upper-layer velocity that is proportional to $(gH\Delta\rho/\rho_0)^{1/2}$. Thus for frictionally- and hydraulically controlled flows, we anticipate that the exchange flow is proportional to uH, that is, proportional to $\Delta\rho^{1/2}H^{3/2}$. By using this result in combination with eq. (5), we obtain a steady-state flow that is proportional to $\Delta\rho^{-2/5}$. Accordingly, the steady-state flow is expected to still decrease with increasing density difference under these slightly different assumptions concerning M_G. We stress, however, that if the vertical diffusivity is taken to be constant, independent of the stratification, the classical thermocline scaling predicts that the flow is proportional to $\Delta\rho^{1/3}$ (e.g. Welander, 1971; Nilsson and Walin, 2001).

3. Analysis of the model: regimes and steady-state features

3.1. *Steady-state solutions in the mixing-limited regime*

We consider first the features of the flow in the mixing-limited regime in a very deep basin where the influence of the sill can be ignored. To analyse the steady-state solutions, we use the following non-dimensional variables

$$(\Delta S_*, H_*, M_*) = (\rho_0\beta\overline{\Delta S}/\Delta\rho_T, \overline{H}/H_T, \overline{M}/M_T), \tag{9}$$

where H_T and M_T are the upper-layer depth and the flow, defined by eqs (7a) and (7b), which result when $\Delta\rho = \Delta\rho_T$. The non-dimensional density difference is given by

$$\Delta\rho_* = \Delta S_* - 1. \tag{10}$$

For the salinity-dominated flows considered in this study $\Delta\rho_* \geq 0$ and $\Delta S_* \geq 1$. In the absence of a salinity stratification, $\Delta\rho_* = -1$, reflecting the unstable thermal stratification. In this situation, a thermally dominated circulation would arise with the surface flow directed into semi-enclosed basin. We do not considered the thermally dominated regime here. However, the thermal density difference $\Delta\rho_T$ is the most convenient quantity to base density and salinity scales on.

Using the definitions introduced above, we obtain the following non-dimensional steady-state relations

$$H_* = (\Delta S_* - 1)^{-2/3}, \tag{11a}$$

$$M_* = (\Delta S_* - 1)^{-1/3}, \tag{11b}$$

$$0 = -\Delta S_* M_* + R. \tag{11c}$$

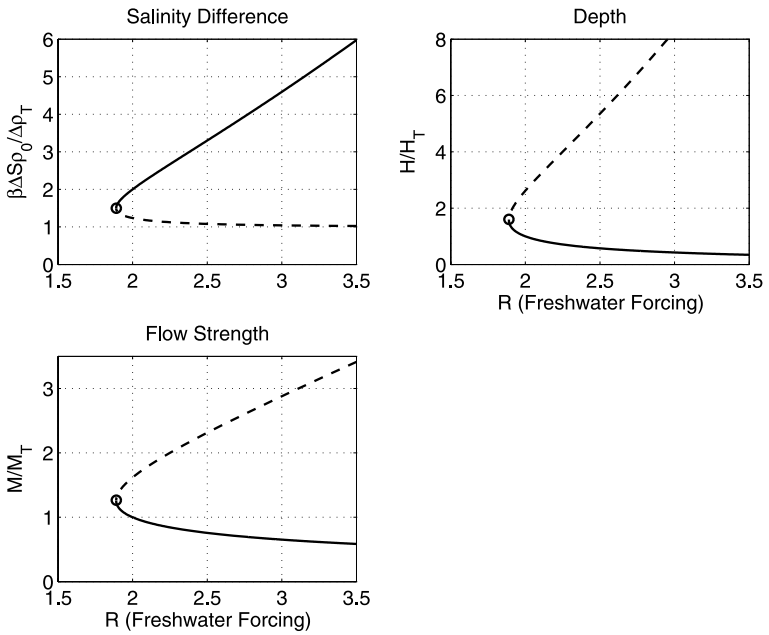

Fig. 3. Equilibrium solutions for the mixing-limited regime, described by eqs (11a)–(11c), as a function of the non-dimensional freshwater supply R; see eq. (12). The solid and dashed lines represent the stable and unstable branches, respectively. Note that influences of the sill are ignored here. The present graph of the flow strength is similar to Fig. 2b in Guan and Huang (2008), which shows the steady-state flow strength as a function of the mixing energy $\mathcal{E}$ in their two-box model; note that $R \propto \mathcal{E}^{-2/3}$ in our model.

Here, the last relation is the steady-state salinity balance and

$$R \equiv \frac{F\beta S_2\rho_0}{M_T\Delta\rho_T}, \tag{12}$$

the non-dimensional freshwater supply. Note that R decreases with increasing mixing energy $\mathcal{E}$, basin area A and thermal density difference $\Delta\rho_T$.

Figure 3 shows the salinity difference, upper-layer depth, and flow strength as a function of the freshwater supply. There is a critical value of R, attained at $\Delta S_* = 3/2$, below which there are no steady states in the mixing-limited regime. The reason is that the steady-state flow strength increases with decreasing salinity difference: For salinity differences smaller than 3/2 the flow becomes so strong that the implied advective freshwater transport exceeds the freshwater supply. This can be contrasted with the Stommel model that allows for salinity-dominated equilibria when the freshwater supply approaches zero (e.g. Marotzke, 2000; Longworth et al., 2005).

To analyse the stability of the steady-state flow, we consider the time evolution of small perturbations resulting from eqs (2a) and (2b)

$$A\frac{\mathrm{d}H'}{\mathrm{d}t} = -M'_G + M'_D, \tag{13a}$$

$$A\overline{H}\frac{\mathrm{d}\Delta S'}{\mathrm{d}t} = -\Delta S'\overline{M} - \overline{\Delta S}M'_D, \tag{13b}$$

where only the terms that are linear in the perturbed quantities, denoted by primes, are retained. A formal stability analysis is undertaken in the Appendix. It shows that at the minimum freshwater supply, one stable and one unstable branch of equilibria merge. The stable branch has stronger density and salinity differences as well as smaller flow rates and upper-layer depths than the unstable branch.

Some qualitative features of the stability can be illuminated be considering the effects of a positive salinity perturbation, which implies an enhanced density difference. The eq. (13b) shows that there are two feedbacks acting on the salinity perturbation: The negative feedback due to the mean-flow advection of the salinity perturbation; and the feedback due to the response of the upwelling M'_D to the salinity perturbation. With the present formulation of M_D, a positive salinity perturbation is associated with a reduced upwelling. In isolation, this constitutes a positive feedback, as weaker upwelling, that is, $M'_D < 0$, acts to amplify the salinity perturbation. However, the decrease of the upwelling will via the continuity relation eq. (13a) act to reduce the upper-layer depth. This represents a stabilizing feedback, which is re-enforced by the response of M'_G, since a reduction of the upper-layer depth act to enhance the upwelling. The formal stability analysis in the Appendix shows that the salinity-dominated flow is stable only if the steady-state salinity difference exceeds a critical value ΔS_{ML} given by

$$\Delta S_{ML} = 3/2. \tag{14}$$

As shown in the Appendix, the value of ΔS_{ML} depends on the details of M_D: For the present parametrization the haline density difference must be 50% larger than the thermal density difference for the flow to be stable. The corresponding critical freshwater supply is obtained from eq. (11c)

$$R_{ML} = \Delta S_{ML}(\Delta S_{ML} - 1)^{-1/3} \approx 1.8. \tag{15}$$

For salinity differences lower than ΔS_{ML}, the positive feedback is stronger than the negative ones due to the mean-flow advection and the adjustments of the upper-layer depth, resulting

in a runaway state where the density contrast approaches zero and the upper-layer depth and the flow strength grow without bound. An interesting question is what type of flow that is established when the mixing-limited flow becomes unstable. One possibility is that a thermally dominated flow emerges after the transients have vanished. In a sill basin, another possibility is that an overmixed salinity-dominated flow is established once the upper layer reaches below the sill. Whether an overmixed flow can exits for low freshwater supplies in the range where no mixing-limited solution exists will now be examined.

3.2. Steady-state solutions in presence of a sill

We now consider how the presence of a sill affects the steady-state properties. By using the eqs (2b) and (8b), the salinity balance for the overmixed flow can be written

$$\Delta S_*(\Delta S_* - 1) = \frac{F\beta S_2 \rho_0}{\Delta\rho_{\rm T}} \frac{2f\rho_0}{g\Delta\rho_{\rm T} D^2}. \tag{16}$$

Here the term on the right-hand side defines another non-dimensional measure of the freshwater supply; see eq. (10). Two features should be emphasized concerning the steady-state salinity balance. First, it is entirely independent of the nature of the small-scale mixing and its associated diapycnal upwelling $M_{\rm D}$ (see also Stommel and Farmer, 1953). Second, as the steady-state flow is linearly proportional to the density difference, that is, $\Delta S_* - 1$, the salinity balance equation is mathematically identical to that of Stommel's two-box model with a prescribed temperature difference (see e.g. Marotzke, 2000). Thus, unlike in the mixing-limited regime, there are steady-state solutions for arbitrary weak freshwater forcing in the overmixed regime. However, there remain two important issues that need to be addressed. First, we need to determine the range of salinity difference for which the upper-layer extends below the sill. Second, the stability of the overmixed steady-state solutions must be examined. For these two issues, the nature of the diapycnal flow will prove to be crucial.

The character of the flow in the sill basin depends primarily on the depth ratio $H_{\rm T}/D$. This new non-dimensional parameter and R govern the steady-state properties. By using the non-dimensional variables defined in eq. (10), the equations governing the overmixed regime can after some algebra be written as

$$H_* = (\Delta S_* - 1)^{-2}(H_{\rm T}/D)^2, \tag{17a}$$

$$M_* = (\Delta S_* - 1)(H_{\rm T}/D)^{-2}, \tag{17b}$$

$$0 = -\Delta S_* M_* + R. \tag{17c}$$

Note that the details of eq. (17a) depend on the nature of the diapycnal flow $M_{\rm D}$, whereas eqs (17b) and (17c) apply for any representation of $M_{\rm D}$; recall that $H_{\rm T}$ is defined as the equilibrium depth that results in the mixing-limited regime when the density difference equals $\Delta\rho_{\rm T}$. A closer inspection reveals that the factor $(H_{\rm T}/D)^{-2}$ always appears in eq. (17b), although different representations of $M_{\rm D}$ can yield different values of $H_{\rm T}$.

To analyse the system, it is convenient to introduce the non-dimensional salinity difference for which the upper layer touches the sill. To obtain this quantity we use eq. (7a) or (8a) to compute the dimensional density for which $H = D$

$$\Delta\rho_{\rm D} \equiv \left(\frac{A\mathcal{E}2\rho_0 f}{g^2 D^3}\right)^{1/2}. \tag{18}$$

Note that $\Delta\rho_{\rm D}$ is independent of the freshwater supply. From the definitions of $\Delta\rho_{\rm T}$ and $H_{\rm T}$, it follows that

$$\Delta\rho_{\rm D}/\Delta\rho_{\rm T} = (H_{\rm T}/D)^{3/2}. \tag{19}$$

The non-dimensional salinity difference for which the upper layer touches the crest of the sill can be written as

$$\Delta S_{\rm D} \equiv \Delta\rho_{\rm D}/\Delta\rho_{\rm T} + 1. \tag{20}$$

Thus, when $\Delta S_* > \Delta S_{\rm D}$, the flow is in the mixing-limited regime described by eqs (11a)–(11c). On the other hand, when $\Delta S_* < \Delta S_{\rm D}$, the flow is in the overmixed regime described by eqs (17a)–(17c).

Let us now consider the stability of the equilibria in the overmixed regime to small perturbations. A somewhat remarkable result is that the flow is stable only if the steady-state salinity exceeds a critical value $\Delta S_{\rm OM}$ given by (see the Appendix)

$$\Delta S_{\rm OM} = 2. \tag{21}$$

Thus, there is a threshold freshwater forcing below which the overmixed salinity-dominated equilibria are unstable

$$R_{\rm OM} = 2(D/H_{\rm T})^2. \tag{22}$$

This behaviour can be contrasted with the salinity-dominated equilibria in the Stommel model, which always are stable. We recall that the present overmixed flow and the Stommel model have the same equilibrium features. However, eq. (13b) shows that the stability of the overmixed flow depends on the physics of the diapycnal flow $M_{\rm D}$, which gives rise to a positive feedback between salinity- and upwelling-perturbations. It is noteworthy that the mixing-limited flow is more stable than the overmixed flow, in the sense that the former remains stable for a smaller steady-state salinity difference, that is, $\Delta S_{\rm ML} < \Delta S_{\rm OM}$. The reason is that in the mixing-limited regime the dependence of the geostrophic outflow $M_{\rm G}$ on the upper-layer depth provides a negative feedback that is absent in the overmixed regime.

Depending on the value of $\Delta S_{\rm D}$, the steady-state response to varying freshwater forcing falls into three categories.

Case A: $\Delta S_{\rm D} < \Delta S_{\rm ML} = 1.5$. The mixing-limited solution is the only salinity-dominated equilibrium solution, which exists in the salinity range $\Delta S_* \geq \Delta S_{\rm ML}$. The maximum upper-layer depth, attained for $R = R_{\rm ML}$, is shallower than the sill and given by $H_* = 0.5^{-2/3} \approx 1.6$.

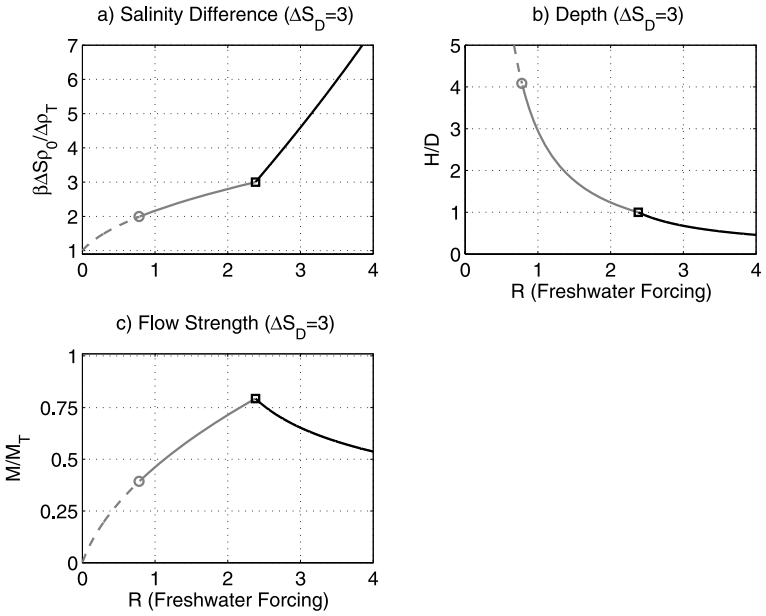

Fig. 4. Equilibrium solutions in the presence of a sill as a function of the non-dimensional freshwater supply R for $\Delta S_{\mathrm{D}} = 3$; see eqs (12) and (20). The grey solid and dotted lines represent the stable and unstable branch of equilibria in the overmixed regime, for which the upper-layer is deeper than the sill, that is, $H > D$. The black solid line represent the stable equilibrium branch in the mixing-limited regime where $H < D$. The square marks the position where $H = D$. At this point, the non-dimensional salinity and density are ΔS_{D} and $\Delta S_{\mathrm{D}} - 1$, respectively.

Case B: $\Delta S_{\mathrm{ML}} < \Delta S_{\mathrm{D}} < \Delta S_{\mathrm{OM}}$. As R is decreased, the mixing-limited flow transits to an unstable overmixed flow when the upper layer touches the crest of the sill. This occurs when $\Delta S_* = \Delta S_{\mathrm{D}}$. The maximum depth for the salinity-dominated flow is the sill depth in this case and there are thus no overmixed equilibrium solutions.

Case C: $2 = \Delta S_{\mathrm{OM}} < \Delta S_{\mathrm{D}}$. In this case, the flow will transit from the mixing-limited to the overmixed regime as the freshwater forcing is decreased. The overmixed flow is now stable and will remain so until $\Delta S_* = \Delta S_{\mathrm{OM}}$. At this stage, the upper-layer depth equals $H_* = (H_{\mathrm{T}}/D)^2$, which is the maximum possible depth for the salinity-dominated flow.

Figure 4 illustrates the latter case, where ΔS_{D} is large enough to admit stable overmixed equilibria for a range of freshwater supplies. Accordingly, as the freshwater supply is reduced below R_D there is a continuous transition from the mixing-limited to the overmixed regime. Note that the dependence of the flow strength on the density difference is reversed in the transition. The maximum flow strength, given by $M_* = (H_{\mathrm{T}}/D)^{-1/2}$, is attained when the upper layer touches the crest of the sill. The fact that the flow becomes weaker when the freshwater forcing increases in the mixing-limited regime, explains why the sensitivity of ΔS_* to changes of R is higher in this regime than in the overmixed one.

Note that there are values of the freshwater supply for which the steady-state solutions of the present model either are unstable or do not exist. In this case, we anticipate that a thermally dominated flow, characterized by a surface flow of buoyant water into the semi-enclosed basin, will be established. However, the resulting thermally dominated steady-state flows, for which $\Delta S_* < 1$, are not considered in this study.

3.3. Multiple equilibrium states?

The present authors originally conjectured that the effects of the sill should stabilize the salinity-dominated flow in the overmixed regime. As shown in the stability analysis, however, the sill serves to destabilize the flow by eliminating the negative feedback due to the dependence of the geostrophic outflow on the upper-layer depth. It should be emphasized that we have assumed that the features of M_{D} are the same regardless whether the upper layer is deeper or shallower than the sill. It is conceivable that $\mathcal{E}$, the rate of work against the buoyancy force per unit area associated with the vertical mixing, does not remain constant when the upper layer extends deep below the sill. Furthermore, we have for the sake of simplicity assumed that the bottom area of the upper layer is a constant independent of H, which amounts to having vertical side boundaries in the basin. The real ocean has sloping side boundaries, and hence, the bottom area of the upper layer $A(H)$ should decrease when the upper-layer depth increases. This causes M_{D}, which is proportional to $A(H)$, to decrease more rapidly with H than when A is taken to be fixed. This strengthens the negative feedback on perturbations of the upper-layer depth and hence acts stabilizing. A similar stabilizing effect results if $\mathcal{E}$ decreases with H. Thus, it is fully possible that overmixed flows in semi-enclosed basins can be more robust than suggested by the present simple model.

To illustrate an interesting dynamical possibility, we consider a hypothetical sill basin where the overmixed salinity-dominated flow remains stable for salinity differences lower than ΔS_{ML}, the critical value below which there exist no mixing-limited equilibria according to the present model. In this case, changes of the boundary conditions can trigger abrupt transitions between mixing-limited and overmixed equilibria provided that the

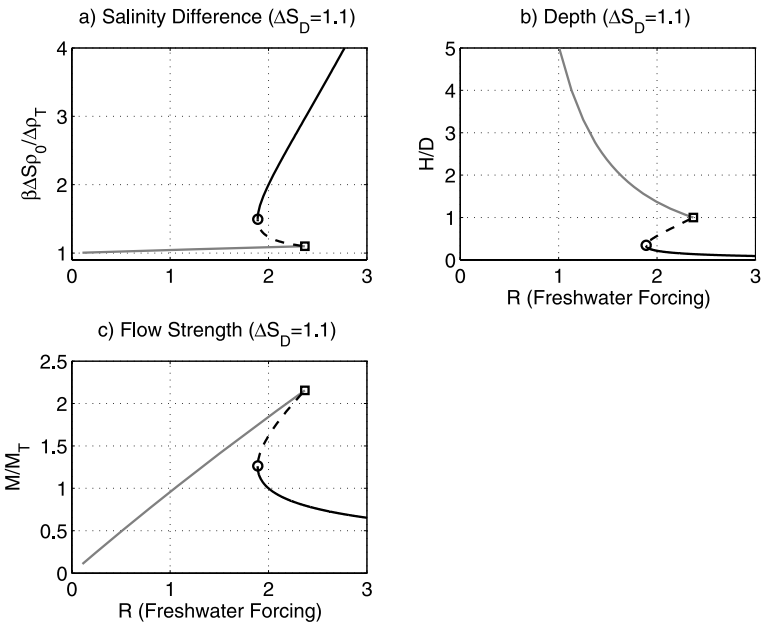

Fig. 5. Equilibrium solutions in the presence of a sill for $\Delta S_{\mathrm{D}} = 1.1$; see eqs (12) and (20). Note that to illustrate the possibility of multiple equilibria, the overmixed flow is assumed to be stable for arbitrarily small freshwater forcing. The grey solid line represents the overmixed branch of equilibria. The black solid and dashed lines represent the stable and unstable equilibrium branches in the mixing-limited regime for which $H \leq D$. The square marks the point $H = D$, where the non-dimensional salinity difference is ΔS_{D}. Provided that $\Delta S_{\mathrm{D}} < \Delta S_{\mathrm{ML}} = 3/2$, there exist multiple equilibrium solutions.

upper layer in the mixing-limited regime is shallower than the sill, that is, $\Delta S_{\mathrm{D}} < \Delta S_{\mathrm{ML}}$. Figure 5 shows a situation associated with abrupt transitions, based on the eqs (17a)–(17c). Note that for the purpose of illustration, we have simply ignored that the overmixed flow is unstable for the present parametrization of M_{D}. In this hypothetical example, the mixing-limited flow will make an abrupt transition to an overmixed equilibrium if the freshwater supply is decreased below R_{ML}. The ensuing overmixed flow is characterized by a weaker salinity difference and larger flow strength and upper-layer depth. By then increasing R, the upper layer of the overmixed flow will gradually rise towards the crest of the sill. When $H = D$, the equilibria in the overmixed regime connect with the unstable branch of equilibria in the mixing-limited regime. As the salinity difference exceeds ΔS_{D}, the upper layer becomes shallower than the sill depth and the flow becomes a mixing-limited equilibrium, which is unstable. Accordingly, the flow will make an abrupt transition to the stable equilibrium solution in the mixing-limited branch. In the hypothetical example, there are multiple equilibrium solutions and hysteresis effects for freshwater supply in the interval $R_{\mathrm{ML}} < R < R_D$.

It is relevant to note that by including salt transport due to horizontal diffusion or wind-forced flow, represented as a constant linear damping of the salinity difference, the salinity-dominated flow is generally stabilized. In the Stommel model as well as for the present overmixed flow, however, a linear damping of the salinity difference acts to remove the salinity-dominated equilibria with very weak circulation and small density difference that arise when the freshwater forcing approaches zero (see Longworth et al., 2005; Guan and Huang, 2008). The reason is that with linear damping included, the salinity tendency does no longer approach zero when the density-dependent flow rate approach zero. Thus, the inclusion of an additional flow component, which is independent of the density difference, should serve to stabilize the present model of the overmixed flow, but there would be a minimum freshwater supply below which no steady-state solutions are found.

4. Discussion

We have examined the dynamics of a salinity-dominated thermohaline circulation in a sill basin using a conceptual two-layer model. A critical model assumption is that the energy supply to the small-scale vertical mixing in the basin is fixed and that the diapycnal upwelling has the same features both when the upper layer is shallower and deeper than the sill. For the mixing-limited regime, where the upper layer is shallower than the sill, there is a critical freshwater forcing below which no steady states exist. This feature is present also in the two-box model of Guan and Huang (2008) and is hinted in numerical simulations presented by Mohammad and Nilsson (2004). When the mixing-limited regime becomes unstable at the critical freshwater forcing, the upper-layer depth of the model is predicted to grow beyond bounds. A central question has been whether the presence of a sill can give rise to a new salinity-dominated steady state for which the upper layer extends below the sill. We found that the dynamical effects due to the sill admit such steady-state solutions for arbitrarily weak freshwater forcing. However, the stability analysis revealed that the overmixed flow becomes unstable below a critical freshwater forcing. Remarkably, the overmixed flow was found to be less robust than the mixing-limited flow, which can remain stable for smaller salinity differences. However, a qualitative examination suggests that topographical effects due to sloping basin boundaries and

modest alterations of the vertical mixing parametrization can serve to stabilize the overmixed flow. Accordingly, it is possible that the salinity-dominated flow in a sill basin may have two stable equilibrium solutions for the same boundary conditions: One overmixed solution with a stronger flow; and one mixing-limited solution with a weaker flow. In a certain parameter range, modest changes of vertical mixing, thermal density difference, or freshwater supply could then trigger abrupt transitions between the two types of equilibria. We have not addressed the possibility that the mixing-limited flow, when it becomes unstable in the sill basin, is succeeded by a forward thermally dominted flow, rather than by a salinity-dominated overmixed flow. We note, however, that Stigebrandt (1985) have analysed some aspect of the thermally dominated flow across the Greenland–Scotland Ridge on the basis of a two-layer model.

We will now discuss some possible oceanographic implications of our model results in the context of the Arctic Ocean. Evidently, our model neglects several important aspects of the Arctic Ocean circulation such as its complex bathymetry, the exchange through the Bering Strait, wind-driven circulation, and the role of the sea ice (see e.g. Stigebrandt, 1981; Rudels, 1995; Nøst and Isachsen, 2003; Rudels et al., 2005). The limitations of our idealized model should be kept in mind in the following qualitative considerations. Based on the present-day conditions, one finds that $A \approx 9 \times 10^{12}\,\mathrm{m}^2$, $\mathcal{E} \approx 10^{-3}\,\mathrm{W\,m}^{-2}$, $F \approx 0.3$ Sv and $\Delta\rho_\mathrm{T} \approx 0.2$ kg m^{-3} (see e.g. Stigebrandt, 1981; Jakobsson, 2002; Jakobsson et al., 2007; Nilsson et al., 2008). Using these values, one obtains the following model quantities: $H_\mathrm{T} \approx 800$ m, $M_\mathrm{T} \approx 6$ Sv and $R \approx 7$. Further, if we assume that the Greenland–Scotland Ridge, with an average depth of about 500 m, serves as the sill for the Arctic, then eq. (20) yields $\Delta S_\mathrm{D} \approx 3$; recall that ΔS_D is the non-dimensional salinity difference for which the upper layer is in level with the sill, which occurs for $R \approx 2.3$. The model features for $\Delta S_\mathrm{D} = 3$ are illustrated in Fig. 4, indicating that the upper-layer depth may reach about 2000 m before the overmixed flow becomes unstable. Under glacial conditions, the freshwater supply is decreased by the general decline of the hydrological cycle as well as by the drying up of the Bering Strait. Accordingly, it seems possible that the freshwater supply becomes weak enough to established an overmixed flow, with a low-salinity upper layer extending below the Greenland–Scotland Ridge. The fact that shelf ice has extended several hundreds of meter below the surface in the Arctic Ocean during glacial periods (Polyak et al., 2001; Jakobsson et al., 2008) supports the notion of a deep cold halocline. Presently, Atlantic Water with temperatures well above freezing is encountered below the cold halocline in the depth range from about 150 to 500 m. The presence of an Atlantic Water layer of present-day characteristics during glacial times would have rapidly melted any deep reaching shelf ice (M. Jakobsson, personal communication 2009).

Another speculative application of the present model concerns the paleo circulation in the Arctic some 20–15 million years ago, a period during which the Fram Strait opened up and gradually became deeper. Jakobsson et al. (2007) present palaeo data and model analyses suggesting that this geological evolution lead to the establishment of a present-day type of circulation in the Arctic Ocean characterized by well-oxygenated deep water. Sediment records from the Central Arctic indicate that in the earlier stages of the Fram Strait opening, there were alternately periods with anoxic- and oxic-conditions in the deeper parts of the basin. Jakobsson et al. (2007) suggest that this reflects changes, forced by sea level variations, between a lake state, ventilated by seasonal convection and a poorly ventilated estuarine circulation reminiscent of the present-day Black Sea. An alternative explanation could be that the oxygen alterations reflect changes between a swift overmixed flow and a slow mixing-limted flow, both being of the estuary type.

In conclusion, we deem that the dynamics of salinity-dominated thermohaline circulations in sill basins such as the Arctic Mediterranean have interesting geophysical and paleo oceanographic applications. However, there remain fundamental questions to be answered concerning the stability of the salinity-dominated flow in the limit of weak freshwater forcing, where the salinity stratification is anticipated to extend to great depths.

5. Acknowledgments

We thank Martin Jakobsson for comments and interesting discussions. We also thank two anonymous reviewers, who provided insightful and constructive suggestions for improving the paper. The work reported here was supported by the Swedish Research Council and is a contribution from the Bert Bolin Centre for Climate Research at Stockholm University.

6. Appendix

We here analyse the linear stability of the equilibrium solutions. To allow for an analysis that encompasses other representations of the diapycnal flow than the one given in eq. (5), we follow Nilsson and Walin (2001) and write $M_\mathrm{D} \propto \Delta\rho^{-\zeta}\, H^{-\eta}$; where $\zeta \geq 0$ and $\eta \geq 0$. The present model of M_D correspond to $\zeta = 1$ and $\eta = 1$. We use the non-dimensional variables defined in eq. (10) and the time scale $AH_\mathrm{T}/M_\mathrm{T}$, which yields the following non-dimensional versions of eqs (13a) and (13b) (without the asterisk notation)

$$\frac{\mathrm{d}H'}{\mathrm{d}t} = -M'_\mathrm{G} + M'_\mathrm{D}, \tag{A1}$$

$$\overline{H}\frac{\mathrm{d}\Delta S'}{\mathrm{d}t} = -\Delta S'\overline{M} - \overline{\Delta S}M'_\mathrm{D}. \tag{A2}$$

In the mixing limited regime, the flow is specified by

$$\Delta\rho = (\Delta S - 1), \quad M_\mathrm{G} = \Delta\rho H^2, \quad M_\mathrm{D} = \Delta\rho^{-\zeta} H^{-\eta}. \tag{A3}$$

In a steady-state $M_G = M_D$, which yield the following steady-state relations

$$\overline{H} = (\overline{\Delta S} - 1)^{(\lambda-1)/2}, \quad \overline{M} = (\overline{\Delta S} - 1)^{\lambda}, \tag{A4}$$

where overbars denote equilibrium-state variables and

$$\lambda \equiv (\eta - 2\zeta)/(\eta + 2). \tag{A5}$$

Thus, the steady-state dependence of the upper-layer depth and the flow strength on the density difference are determined by the parameter λ. When M_D is given by eq. (5), $\lambda = -1/3$; see Nilsson and Walin (2001) for results concerning other representations of M_D. The linearized perturbations are given by

$$\begin{aligned} \Delta\rho' &= \Delta S', \quad M'_G = [(\Delta\rho'/\overline{\Delta\rho}) + 2(H'/\overline{H})]\overline{M}, \\ M_D &= -[\zeta(\Delta\rho'/\overline{\Delta\rho}) + \eta(H'/\overline{H})]\overline{M}. \end{aligned} \tag{A6}$$

The eqs (A1) and (A2) can be written on the form

$$\frac{\mathrm{d}}{\mathrm{d}t}\begin{pmatrix} H' \\ \Delta S' \end{pmatrix} = \begin{pmatrix} a & b \\ c & d \end{pmatrix}\begin{pmatrix} H' \\ \Delta S' \end{pmatrix}, \tag{A7}$$

where the coefficients in the stability matrix are given by

$$a \equiv -\overline{H}(\overline{\Delta S} - 1)(2 + \eta), \quad b \equiv -\overline{H}^2(1 + \zeta),$$

$$c \equiv \eta\overline{\Delta S}(\overline{\Delta S} - 1), \quad d \equiv \overline{H}[1 + \overline{\Delta S}(\zeta - 1)].$$

We seek solutions on the form $\exp(\sigma t)$ and (A7) determines the exponents

$$\sigma_{1/2} = \frac{a+d}{2} \pm \left[\frac{(a+d)^2}{2} + bc - ad\right]^{1/2}. \tag{A8}$$

An equilibrium solution is stable if $a + d < 0$ and $bc - ad < 0$. The condition $a + d < 0$ is satisfied if

$$\overline{\Delta S} > (3 + \eta)/(3 + \eta - \zeta). \tag{A9}$$

By using the definition of λ, the second stability condition can be expressed as $[1 - \overline{\Delta S}(1 + \lambda)] < 0$. When $\lambda > 0$, this condition is always satisfied for the salinity-dominated flow since $\overline{\Delta S} > 1$. When $\lambda < 0$. On the other hand, the condition is only satisfied if

$$\overline{\Delta S} > 1/(1 + \lambda) \equiv \Delta S_{ML}. \tag{A10}$$

In the present model, where $\zeta = 1$ and $\eta = 1$, the stability is determined by eq. (A10), which yields $\Delta S_{ML} = 3/2$.

The difference in the overmixed regime is that the geostrophic flow and its perturbation are given by

$$M_G = \Delta\rho(D/H_T)^2, \quad M'_G = \Delta\rho'(D/H_T)^2 = (\Delta\rho'/\overline{\Delta\rho})\overline{M}, \tag{A11}$$

where the steady-state flow is given by

$$\overline{M} = \overline{\Delta\rho}(D/H_T)^2 = \overline{\Delta\rho}^{-1}\overline{H}^{-1}, \tag{A12}$$

where we have used the the eqs (17a) and (17b).

In the overmixed regime, straightforward calculations show that the coefficients in the stability matrix are given by

$$a \equiv -\eta(\overline{\Delta S} - 1)/\overline{H}, \quad b \equiv -(1 + \zeta),$$

$$c \equiv \eta\overline{\Delta S}(\overline{\Delta S} - 1)/\overline{H}^2, \quad d \equiv [1 + \overline{\Delta S}(\zeta - 1)]/\overline{H}.$$

Here, the condition that $bc - ad < 0$ yields the criteria

$$\overline{\Delta S} > 1/2, \tag{A13}$$

which is always satisfied for salinity-dominated flows. The condition that $a + d < 0$, yields the criteria

$$\overline{\Delta S} > (1 + \eta)/(1 + \eta - \zeta) \equiv \Delta S_{OM}. \tag{A14}$$

This criteria determines the stability of the overmixed flow; it shows that by increasing η the flow becomes more stable in the sense that the critical salinity ΔS_{OM} is lowered. Thus, if M_D decreases sharply with H, the flow becomes more stable. In the present model, where $\zeta = 1$ and $\eta = 1$, we find that $\Delta S_{OM} = 2$.

References

Aaboe, S. and Nøst, O.-A. 2008. A diagnostic model of the Nordic Seas and Arctic Ocean circulation: quantifying the effects of a variable bottom density along a sloping topography. *J. Phys. Oceanogr.* **38**, 2685–2703.

Bryan, F. 1987. Parameter sensitivity of primitive equation ocean general circulations models. *J. Phys. Oceanogr.* **17**, 970–985.

Gnanadesikan, A. 1999. A simple predictive model for the structure of the oceanic pycnocline. *Science* **283**, 2077–2079.

Greenspan, H. P. 1968. *The Theory of Rotating Fluids* 1st Edition. Cambridge University Press, Cambridge, UK.

Guan, Y. G. and Huang, R. X. 2008. Stommel's box model of thermohaline circulation revisited—the role of mechanical energy supporting mixing and the wind-driven gyration. *J. Phys. Oceanogr.* **38**, 909–917.

Huang, R. X. 1999. Mixing and energetics of the oceanic thermohaline circulation. *J. Phys. Oceanogr.* **29**, 727–746.

Iovino, D., Straneo, F. and Spall, M. 2008. On the effect of a sill on dense water formation in a marginal sea. *J. Mar. Res.* **66**, 325–345.

Jakobsson, M. 2002. Hypsometry and volume of the Arctic Ocean and its constituent seas. *Geochem. Geophys. Geosyst.* **3**, 1–18.

Jakobsson, M., Backman, J., Rudels, B., Nycander, J., Frank, M. and co-authors. 2007. The early Miocene onset of a ventilated circulation regime in the Arctic Ocean. *Nature* **447**, 986–990.

Jakobsson, M., Polyak, L., Edwards, M. and Coakley, J. K. B. 2008. Glacial geomorphology of the Central Arctic Ocean: the Chukchi Borderland and the Lomonosov Ridge. *Earth Surf. Process. Landforms* **33**, 526–545.

Kato, H. and Phillips, O. M. 1969. On the penetration of a turbulent layer into a stratified fluid. *J. Fluid Mech.* **37**, 643–655.

Kuhlbrodt, T., Griesel, A., Montoya, M., Levermann, A., Hofmann, M. and co-authors. 2007. On driving processes of the Atlantic meridional overturning circulation. *Rev. Geophys.* **45**, doi:10.1029/2004RG000166.

Longworth, H., Marotzke, J. and Stocker, T. F. 2005. Ocean gyres and abrupt change in the thermohaline circulation: a conceptual analysis. *J. Climate* **18**, 2403–2416.

Lyle, M. 1997. Could early Cenozoic thermohaline circulation have warmed the poles? *Paleoceanography* **12**, 161–167.

Marchal, O., Jackson, C., Nilsson, J., Paul, A. and Stocker, T. F. 2007. Buoyancy-driven flow and nature of vertical mixing in a zonally-averaged model. In: *Past and Future Changes of the Ocean's Meridional Overturning Circulation: Mechanisms and Impacts* Volume 173 (eds A. Schmittner, J. Chiang, and S. Hemming). AGU Geophysical Monograph, American Geophysical Union, Washington, DC, 33–52.

Marotzke, J., 1996. Analysis of thermohaline feedbacks. In: *Decadal Climate Variability; Dynamics and Predicatbility* (eds D. L. T. Anderson, and J. Willebrand). Volume I , 44 NATO ASI Series, Springer-Verlag, Heidelberg, Germany, 334–378.

Marotzke, J. 2000. Abrupt climate change and the thermohaline circulation: mechanisms and predictability. *P. Natl. Acad. Sci. U.S.A.* **97**, 1347–1350.

Marshall, J. and Radko, T. 2006. A model of the upper branch of the meridional overturning of the southern ocean. *Prog. in Oceanogr.* **70**, 331–345.

Mohammad, R. and Nilsson, J. 2004. The role of diapycnal mixing for the equilibrium response of thermohaline circulation. *Ocean Dyn.* **54**, 54–65.

Mohammad, R. and Nilsson, J. 2006. Symmetric and asymmetric modes of the thermohaline circulation. *Tellus* **58A**, 616–627.

Nilsson, J., Björk, G., Rudels, B., Winsor, P. and Torres, D. 2008. Liquid freshwater transport and Polar Surface Water characteristics in the East Greenland Current during the AO-02 oden expedition. *Prog. Oceanogr.* **78**, 45–57.

Nilsson, J., Broström, G. and Walin, G. 2003. The thermohaline circulation and vertical mixing: does weaker density stratification give stronger overturning? *J. Phys. Oceanogr.* **33**, 2781–2795.

Nilsson, J. and Walin, G. 2001. Freshwater forcing as a booster of thermohaline circulation. *Tellus* **53A**, 629–641.

Nilsson, J., Walin, G. and Broström, G. 2005. Thermohaline circulation induced by bottom friction in sloping-boundary basins. *J. Mar. Res.* **63**, 705–728.

Nøst, O. A. and Isachsen, P. E. 2003. The large-scale time-mean ocean circulation in the Nordic Seas and the Arctic Ocean estimated from simplified dynamics. *J. Mar. Res.* **61**, 175–210.

Park, Y.-G. 1999. The stability of thermohaline circulation in a two-box model. *J. Phys. Oceanogr.* **29**, 3101–3110.

Park, Y.-G. and Bryan, K. 2000. Comparison of thermally driven circulation from a depth-coordinate model and an isopycnal model. Part I: scaling-law sensitivity to vertical diffusivity. *J. Phys. Oceanogr.* **30**, 590–605.

Polyak, L., Edwards, M. H., Coakley, B. J. and Jakobsson, M. 2001. Ice shelves in the Pleistocene Arctic Ocean inferred from glaciogenic deep-sea bedforms. *Nature* **410**, 453–457.

Pratt, L. J. and Spall, M. A. 2008. Circulation and exchange in choked marginal seas. *J. Phys. Oceanogr.* **38**, 2639–2661.

Rudels, B. 1995. The thermohaline circulation of the Artic Ocean and the Greenland Sea. *Phil. Trans. R. Soc. Lond.* **352**, 287–299.

Rudels, B., Björk, G., Lake, I., Nohr, C., Nilsson, J. and co-authors. 2005. The interaction between waters from the Arctic Ocean and the Nordic Seas north of the Fram Strait and along the East Greenland Current: results from the AO-02 Oden expedition. *J. Mar. Syst.* **55**, 1–30.

Spall, M. A. 2004. Boundary currents and water mass transformation in marginal seas. *J. Phys. Oceanogr.* **34**, 1197–1213.

Stigebrandt, A. 1981. A model for the thickness of and salinity of the upper layer in the Arctic Ocean and the relationship between the ice thickness and some external parameters. *J. Phys. Oceanogr.* **11**, 1407–1422.

Stigebrandt, A. 1985. On the hydrographic and ice conditions in the northern North Atlantic during different phases of a glaciation cycle. *Palaeogeogr., Palaeoclimatol., Palaeoecol.* **50**, 303–321.

Stommel, H. M. 1961. Thermohaline convection with two stable regimes of flow. *Tellus* **13**, 224–230.

Stommel, H. M. and Farmer, H. G. 1953. Control of salinity in an estuary by a transition. *J. Mar. Res.* **12**, 13–20.

Thual, O. and McWilliams, J. C. 1992. The catastrophe structure of thermohaline convection in a two-dimensional fluid model and comparison with low-order box models. *Geophys. Astrophys. Fluid Dyn.* **64**, 67–95.

Walin, G. 1985. The thermohaline circulation and the control of ice ages. *Palaeogeogr., Palaeoclimatol., Palaeoecol.* **50**, 323–332.

Walin, G. 1990. On the possibility of a reversed thermohaline circulation. In: *Nordic Perspectives on Oceanography* (ed. P. Lundberg).Kungl. Vetenskaps- och Vitterhets-Samhället i Göteborg., (Available from the author, Earth Science Center, Göteborg University, Box 460, 40530 Göteborg, Sweden), 145–154.

Walin, G., Broströ m, G., Nilsson, J. and Dahl, O. 2004. Baroclinic boundary currents with downstream decreasing buoyancy: a study of an idealized Nordic Sea system. *J. Mar. Res.* **62**, 517–543.

Welander, P. 1971. The thermocline problem. *Phil. Trans. R. Soc. Lond. A.* **270**, 415–421.

Welander, P. 1986. Thermohaline effects in the ocean circulation and related simple models. In: *Large-Scale Transport Processes in the Oceans and Atmosphrere* (eds J. Willebrand, and D. L. T. Anderson). D. Reidel Publishing Company, Dordrecht, The Netherlands, 163–200.

Zhang, J., Schmitt, R. W. and Huang, R. X. 1999. The relative influence of diapycnal mixing and hydrological forcing on the stability of thermohaline circulation. *J. Phys. Oceanogr.* **29**, 1096–1108.